# Mean-field theory of echo state networks

Marc Massar[1] and Serge Massar[2]
[1]*370 Central Park West, Apt. 511, New York 10025 New York, USA*
[2]*Laboratoire d'Information Quantique, CP 225, Université libre de Bruxelles (U.L.B.), Av. F. D. Roosevelt 50, B-1050 Bruxelles, Belgium*
(Received 1 November 2012; revised manuscript received 13 March 2013; published 18 April 2013)

Dynamical systems driven by strong external signals are ubiquitous in nature and engineering. Here we study "echo state networks," networks of a large number of randomly connected nodes, which represent a simple model of a neural network, and have important applications in machine learning. We develop a mean-field theory of echo state networks. The dynamics of the network is captured by the evolution law, similar to a logistic map, for a single collective variable. When the network is driven by many independent external signals, this collective variable reaches a steady state. But when the network is driven by a single external signal, the collective variable is non stationary but can be characterized by its time averaged distribution. The predictions of the mean-field theory, including the value of the largest Lyapunov exponent, are compared with the numerical integration of the equations of motion.

DOI: 10.1103/PhysRevE.87.042809 PACS number(s): 89.75.Hc, 05.45.−a, 87.10.−e, 89.75.Fb

## I. INTRODUCTION

Our understanding of nonlinear dynamical systems and networks has made tremendous progress during the past decades. In most cases the autonomous dynamics is studied. The situation where the network is strongly driven by an external signal has so far been less investigated even though it arises in many different contexts in the natural and artificial world. Examples include networks of interacting chemicals (e.g., proteins and RNA) in a cell driven by unpredictable external chemical signals, networks of neurons driven by an external sensory input, artificial neural networks and their applications in machine learning, the response of population dynamics and ecological networks to changes in external conditions such as the weather, and the responses of stock prices to economically significant news such as a company earnings or unemployment numbers. In all these cases, taking into account the external input is essential if one wants to understand correctly the dynamics, because the external input is often large (it cannot be treated as a small perturbation) and because, in some cases, the system itself has been selected according to its response to the fluctuating and unpredictable external variables.

The aim of the present work is to show, through the study of a specific but important example, how mean-field techniques can provide a detailed understanding of dynamical networks strongly driven by an external signal. In the mean-field approach the average feedback of the variables on themselves is taken into account through a self-consistent equation, while the correlations between individual variables are neglected. The apparently extremely complicated dynamics of the network is thus reduced to much simpler evolution equations for a few collective variables. Previous applications of the mean-field approach to dynamical systems (but without including an external input), and in particular neural networks, include, e.g., Refs. [1–5]. For previous studies of dynamical systems in the presence of external signals (with, however, a different emphasis than in the present work) see, e.g., Refs. [6–8]. Mean-field analysis of multipopulation neural networks in the presence of stochastic noise have been recently presented in Refs. [9,10].

The specific system we will consider is taken from the field of artificial neural networks. It consists of a network of randomly connected idealized neurons evolving in discrete time and driven by an external time-dependent signal, known in the machine learning community as an "echo state network" [11,12]; see also the continuous time analog with no input studied in Ref. [5]. Such systems, when supplemented by a single linear output layer, fall within the class of "reservoir computers" [11–14] and currently hold records for several highly nontrivial machine learning tasks such as time series prediction or some speech recognition benchmarks; see, e.g., Ref. [15] for a review. Because of their importance in the machine learning community, it is highly desirable to better understand the dynamics of these systems. In addition, they can serve as toy models for investigating the dynamics of neural networks, and, more generally, any recurrent dynamical systems, driven by external inputs.

Here we show that the dynamics of echo state networks can be concisely described by a single collective variable, namely the variance $\sigma^2(t)$ of the variables describing the echo state network. In the limit when the number of internal variables is large (which is the case in reservoir computing applications), the variance obeys a closed evolution equation, similar to the logistic map but with a source term (due to the source term that drives the echo state network). We further show how to derive the onset of chaos in echo state networks, and we derive the Lyapunov exponent. In the case of a sigmoid nonlinearity it can be shown that the external input stabilizes the system, as is well known in the community working on echo state networks (see, e.g., Ref. [16]). We note that Lyapunov exponents for dynamical systems driven by stochastic noise were studied in Ref. [17] where it was shown that the noise can dramatically change the stability of the system. Stabilization of chaotic systems by controlled inputs was described in Ref. [18]. Throughout our work we compare in the figures the predictions of the mean-field theory with the exact integration of the equations of motion. In all cases we find excellent agreement.

## II. ECHO STATE NETWORKS

An echo state network consists of a large number $N$ of artificial neurons evolving in discrete time $t \in \mathbb{Z}$. We denote by $a_i(t)$ the "activation potential" of neuron $i$ at time $t$. At

 

time $t+1$, neuron $i$ sends a signal to the other neurons with strength $x_i(t+1)$ given by

$$x_i(t+1) = f(a_i(t)), \tag{1}$$

where the function $f$ is taken to be a sigmoidal functions, i.e., $f$ is odd, monotonously increasing, has finite limit for large $a$, and its first derivative $f'(a)$ decreases monotonously for positive $a$. By rescaling $x$ and $a$ we can redefine $f(a) \to \alpha f(\beta a)$. We choose the scales such that $f'(0) = 1$ and $\lim_{a\to\infty} f(a) = 1$. In the illustrative figures, we choose for $f$ the hyperbolic tangent $f(a) = \tanh(a)$, as this is the form most often used in echo state networks.

The update rule for the activation potentials is

$$a_i(t) = \sum_{j=1}^{N} w_{ij} x_j(t) + u_i s(t), \tag{2}$$

where $w_{ij}$ is a time-independent coupling matrix which gives the strength of the coupling of neuron $j$ to neuron $i$, $s(t)$ is the time-dependent external input, and $u_i$ is a time-independent vector which determines the strength with which the input is coupled to neuron $i$.

In echo state networks, the $w_{ij}$ and $u_i$ are chosen independently at random, except for global scaling factors $w_{ij} \to \mu w_{ij}$, $u_i \to \nu u_i$. By adjusting these scaling factors and by using an optimized linear readout it is possible to obtain excellent performance on a variety of machine learning tasks. The general heuristic is that the factor $\mu$ should be adjusted for the system to be at the threshold of chaos, whereupon the response of the neural network to the input is highly complex but deterministic. Previous studies of the dynamics of echo state networks have aimed to understand how different dynamical regimes are related to changes in their information processing capability [19]. Most closely connected to the present work is Ref. [20] where, based on earlier work on feed-forward networks [21], the information processing capability of echo state networks could be studied in the limit where the number $N$ of neurons tends to infinity.

## III. VARIATIONS AROUND THE ECHO STATE NETWORK EQUATIONS

The echo state network equations (1) and (2) can be modified in a number of ways, all of which are also amenable to treatment using the mean-field approximation. Comparison between these different dynamical systems helps understand the generality but also limitations of the mean-field approximation. We list here the most important such generalizations. In all cases Eq. (1) is unchanged. It is the update rule for the activation potential Eq. (2) that is modified.

### A. Multiple inputs

In some applications of echo state networks, such as, e.g., preprocessed speech signals or image processing, there are multiple inputs $s_1(t), \ldots, s_K(t)$ that drive the system. This is also important in, e.g., spatiotemporal processing by the cortex [22]. We model the multiple inputs $s_l$ as independent random variables.

In this case the update rule for the activation potential becomes

$$a_i(t) = \sum_{j=1}^{N} w_{ij} x_j(t) + \sum_{l=1}^{K} u_{il} s_l(t), \tag{3}$$

where $w_{ij}$ and $u_{il}$ are time-independent coefficients.

### B. Independent inputs

When $K \to \infty$ then the source terms in Eq. (3) become independent random variables (provided the $u_{il}$ are rescaled to keep the variance of the source term finite), and the update rule for the activation potential becomes

$$a_i(t) = \sum_{j=1}^{N} w_{ij} x_j(t) + s_i(t), \tag{4}$$

where $w_{ij}$ are time-independent coefficients and the $s_i$ are independent random variables. This case has been studied previously in Ref. [6].

### C. Annealing approximation

In the annealing approximation (see, e.g., Refs. [23,24] in the case of discrete variables), the update rule for the activation potential is

$$a_i(t) = \sum_{j=1}^{N} w_{ij}(t) x_j(t) + u_i(t) s(t), \tag{5}$$

where $w_{ij}(t)$ and $u_i(t)$ are time-dependent coefficients that, at each time $t$, are drawn independently at random from the same distribution. In the annealing approximation any structure arising from the fixed values of the coefficients $w_{ij}$ and $u_i$ is erased, since these coefficients change at each time $t$. The annealing approximation can be equally applied to the case of multiple inputs [Eq. (3)] and independent inputs [Eq. (4)].

The mean-field approach (discussed in the remainder of this article) can be equally applied in the case of the annealing approximation. The resulting equations are identical to those obtained from Eqs. (1)–(4), that is, the mean-field approach cannot reveal structure that arises from the fixed values of the coefficients $w_{ij}$ and $u_{il}$.

## IV. MEAN-FIELD APPROXIMATION

### A. Mean-field equations

The key insight behind the present work is to make the assumption that, at each time $t$, the $x_i(t)$ behave as independent identically distributed random variables which are also independent of the $w_{ij}$ and the $u_i$. The term $\sum_{j=1}^{N} w_{ij} x_j(t)$ in Eq. (2) then is a sum of many identically distributed independent variables, and the law of large numbers tells us that this sum is distributed as a Gaussian (see Fig. 1).

With this assumption we can compute the distribution of $a_i(t)$ and then, using Eq. (1), the distribution of $x_i(t+1)$. This analysis will yield a very simple one-dimensional recurrence, similar to the logistic map, which captures the essence of the dynamics of the echo state network.

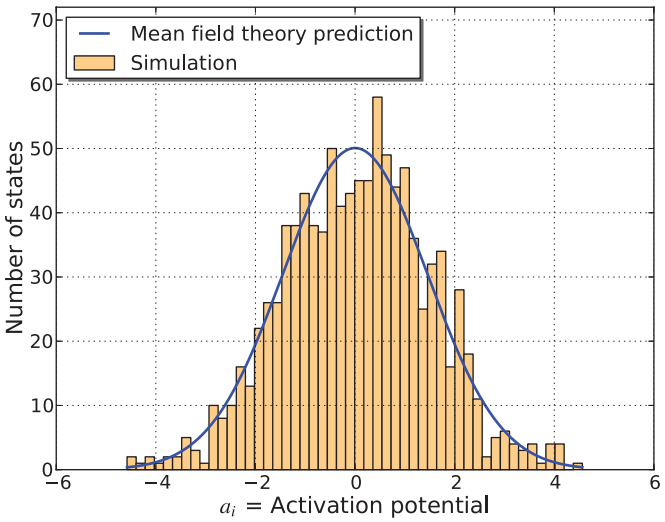


FIG. 1. (Color online) Distribution of the activation potential $a_i$. A reservoir with size $N = 1000$ and normalized gain of $g = 2$ and no source was run for 200 time steps, and then the histogram of the activation potential was plotted in light orange. For comparison, a Gaussian with the variance predicted by the mean-field theory was plotted (solid blue line).

In more detail, we reason as follows. Because the function $f$ is odd, the distribution from which are drawn the $x_i(t)$ has mean zero $\langle x_i(t)\rangle = 0$, where $\langle\rangle$ denotes ensemble average, i.e., average over the index $i$ at fixed time $t$. We denote the variance of the $x_i(t)$ by $\langle x_i^2(t)\rangle = \sigma^2(t)$. Assuming that the $w_{ij}$ are drawn independently at random from a distribution with mean zero $E[w_{ij}] = 0$ and variance $E[w_{ij}^2] = w^2$, and introducing the rescaled gain $g$ as

$$g^2 = Nw^2,$$

we find that the term

$$\sum_{j=1}^{N} w_{ij}x_j(t) \sim N(0, g^2\sigma^2(t))$$

has Gaussian distribution. We now assume for simplicity that the $u_i$ are drawn independently at random from a Gaussian distribution with zero mean and variance $u^2$,

$$u_i \sim N(0,u^2).$$

The activation potential

$$\begin{aligned} a_i(t) &= \sum_{j=1}^{N} w_{ij}x_j(t) + u_i s(t) \\ &\sim N[0, g^2\sigma^2(t) + u^2 s^2(t)] \end{aligned}$$

then also has a Gaussian distribution. (If the $u_i$ are drawn from a distribution other than Gaussian, then the distribution of the $a_i(t)$ can in principle be calculated, but the expressions will be more complicated.) For future use we denote the variance of the $a_i(t)$ as

$$\Sigma^2(t) = g^2\sigma^2(t) + u^2 s^2(t).$$

Finally, the distribution of $x_i$ at time $t+1$ is given by

$$x_i(t+1) \sim f(N(0, \Sigma^2(t))).$$

We thus obtain a closed one-dimensional recurrence for the variances of $x_i(t)$ and $a_i(t)$:

$$\begin{aligned} \Sigma^2(t) &= g^2\sigma^2(t) + u^2 s^2(t), \\ \sigma^2(t+1) &= F(\Sigma^2(t)), \end{aligned} \tag{6}$$

where

$$\begin{aligned} F(\Sigma^2) &= \int da\ f^2(a) \frac{\exp\left[-\frac{a^2}{2\Sigma^2}\right]}{\sqrt{2\pi\,\Sigma^2}} \\ &= \int dy\ f^2(\Sigma y)\ \frac{\exp\left[-\frac{y^2}{2}\right]}{\sqrt{2\pi}}. \end{aligned} \tag{7}$$

From the properties of the sigmoid funtion $f$ (given below Eq. (1)), it follows that $F(\Sigma^2)$ satisfies $F(0) = 0$, $F(+\infty) = 1$, $dF/d\Sigma^2 > 0$, and $dF/d\Sigma^2(\Sigma^2 = 0) = 1$.

In the illustrative figures discussed below we take $f(a) = \tanh(a)$, as this is the case most used in applications of echo state networks. The integral Eq. (7), yielding the stationary solution $F$, must then be carried out numerically (this can be done very efficiently).

It is, however, interesting to note that the function $F(\Sigma^2)$ can be computed analytically in two cases. The first does not correspond to a sigmoid function $f$, but it is of interest as it has been used in a recent experimental implementation of reservoir computing [25,26]: if $f(a) = \sqrt{2}\sin(\frac{a}{\sqrt{2}})$, then $F(\Sigma^2) = 1 - \exp(\Sigma^2)$. The second case is the sigmoidal function $f(a) = \mathrm{erf}(\frac{\sqrt{\pi}}{\sqrt{2}}a)$, whereupon $F(\Sigma^2) = -1 + \frac{4}{\pi}\arctan(\sqrt{1+2\Sigma^2})$ (obtained by first evaluating $\frac{dF(\Sigma^2)}{d\Sigma^2}$, see Ref. [21]). Results for these cases are similar to those when $f(a) = \tanh(a)$ and also show very good agreement between the mean-field approximation and the integration of the exact Eqs. (1) and (2). (Figures for these cases are not shown.)

### B. Solution of the mean-field equations

We now consider the solutions of the mean-field equations, i.e., the coupled one-dimensional recurrence [Eq. (6)]. We first consider the case when there is no source, $s^2 = 0$. When $g < 1$, there is a single stationary solution to Eq. (6), $\sigma^2 = \Sigma^2 = 0$, corresponding to a quiescent system; $g = 1$ corresponds to a branching point. When $g > 1$, the stable stationary solution of Eq. (6) differs from zero: $\sigma^2 > 0$, $\Sigma^2 > 0$. We will see below that when $g > 1$, not only is $\Sigma^2 > 0$ but the Lyapunov exponent of the system Eqs. (1) and (2) is greater than 1. This, therefore, corresponds to a chaotic regime. In the limit of infinite gain $g \to \infty$, we have $\sigma^2 \to 1$, $\Sigma^2 \to g^2$.

When the source $s(t)$ is nonzero, integrating the recurrence Eq. (6) yields a distribution of values for $\sigma^2$ and $\Sigma^2$. In the figures, we take for illustrative purposes the $s(t)$ to be independently drawn at each time $t$ from the same probability distribution, that is, we assume there are no temporal correlations between successive values of the source. For definiteness we take the source

$$s(t) \sim N(0,s^2)$$

to be distributed according to a Gaussian with zero mean and variance $s^2$. We denote

$$\xi^2 = u^2 s^2.$$

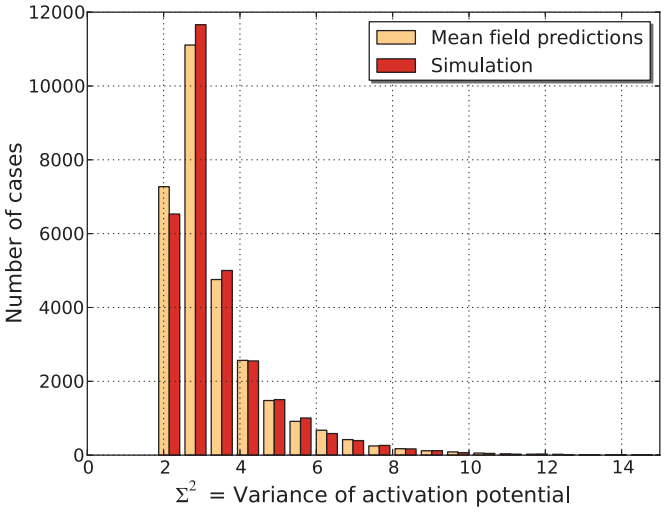


FIG. 2. (Color online) Histogram of the variance $\Sigma^2$ of the activation potential in the presence of source. A reservoir of size $N = 500$ with normalized gain $g = 2$ and a single independent and identically distributed normal source with variance $\xi^2 = 1$ was run for 200 time steps to remove the influence of the initial state. The reservoir then was run for 30 000 time steps, the variance of the activation potential $\Sigma^2(t)$ was collected, and its histogram is plotted in dark gray (red). The same procedure was done following the mean-field theory prediction of Eq. (2) and plotted in light gray (orange).

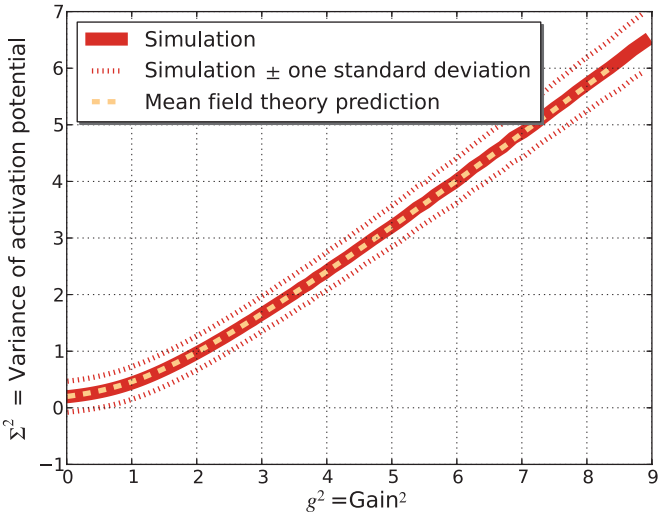


FIG. 3. (Color online) Variance of the activation potential $\Sigma^2$ as a function of normalized gain $g$. For each activation potential, a reservoir of size $N = 500$ with a single independent and identically distributed Gaussian source with variance $\xi^2 = 0.2$ was run according to Eqs. (1) and (2) for 200 time steps to eliminate transitory effects, and then the variance $\Sigma^2(t)$ of the activation potential was recorded for 2000 time steps. For each gain, the mean and standard deviation (over time) of $\Sigma^2(t)$ was computed. The mean is plotted with a solid gray (red) line, and the mean ± one standard deviation are plotted with a dotted gray (red) line. The light gray (orange) dashed curve [superimposed on the solid gray (red) curve in the figure] corresponds to the predictions of the mean-field theory computed according to Eq. (6). The asymptotic behaviors discussed in Sec. IV C, $\lim_{g^2\to 0} \Sigma^2 = \xi^2 = 0.2$ and $\lim_{g^2\to\infty} \Sigma^2 = g^2$, are clearly visible on the graph.

Comparison of the mean-field theory and the exact distribution for $\sigma^2(t)$ obtained by integrating the equations of motion is given in Fig. 2. In Fig. 3 we find excellent agreement between the mean-field theory predictions and the exact solutions for the mean (over time) of $\Sigma^2(t)$ for input strength $\xi^2 = 0.2$ as a function of $g^2$. The asymptotic behaviors $\lim_{g^2\to 0} \Sigma^2 = \xi^2 = 0.2$ and $\lim_{g^2\to\infty} \Sigma^2 = g^2$ are clearly visible on the graph.

### C. Mean-field equations in the case of multiple inputs

We now consider the mean-field approximation in the case where there are multiple inputs Eq. (3) and independent inputs Eq. (4). The new features that arise in this case can be understood qualitatively as follows. When there is a single input $s(t)$, then if, at some time $t$, $s(t)$ is large (small), then the $a_i(t)$ will have a larger (smaller) absolute value than its average, and $\Sigma^2(t)$ will be larger (smaller). Thus, $\Sigma^2(t)$ fluctuates in time. When there are $K$ independent inputs, the same phenomenon occurs but is less pronounced since the fluctuations of the different inputs $s_l(t)$ tend to counterbalance each other. In the limit when there are infinitely many inputs, or, equivalently, when all the inputs are independent, the time-dependent fluctuations of the individual inputs completely average out when we compute $\Sigma^2(t)$, which becomes time independent.

To analyze the case of multiple inputs, we take the coefficients $u_{il}$ to be independent random variables drawn from a normal distribution,

$$u_{il} \sim N(0,u^2).$$

We take the source terms $s_l(t)$ to be independent random variables, with zero mean and variance,

$$s^2 = \mathrm{var}[s_l(t)].$$

We denote by

$$\xi^2 = K u^2 s^2$$

the variance of the source term $\sum_{l=1}^{K} u_{il} s_l(t)$.

The reasoning leading to the mean-field equations then can be followed exactly as in Sec. IV A and one finds the same equations:

$$\begin{aligned} \Sigma^2(t) &= g^2\sigma^2(t) + v_K^2(t) \\ \sigma^2(t+1) &= F(\Sigma^2(t)). \end{aligned} \tag{8}$$

The dependence on the number $K$ of inputs appears only in the source term $v_K(t)$, which is a sum of $K$ squares of Gaussians. It therefore is distributed as a chi-squared with $K$ degrees of freedom,

$$v_K^2(t) \sim u^2 s^2 \chi^2(K),$$

with expectation and variance

$$E\left[v_K^2(t)\right] = \xi^2, \quad \mathrm{var}\left[v_K^2(t)\right] = 2Ku^4s^4 = \frac{2\xi^4}{K}$$

(where the expectations are time averages).

Thus, if we keep the strength of the source term constant, that is, if we keep $\xi^2$ constant but increase the number of

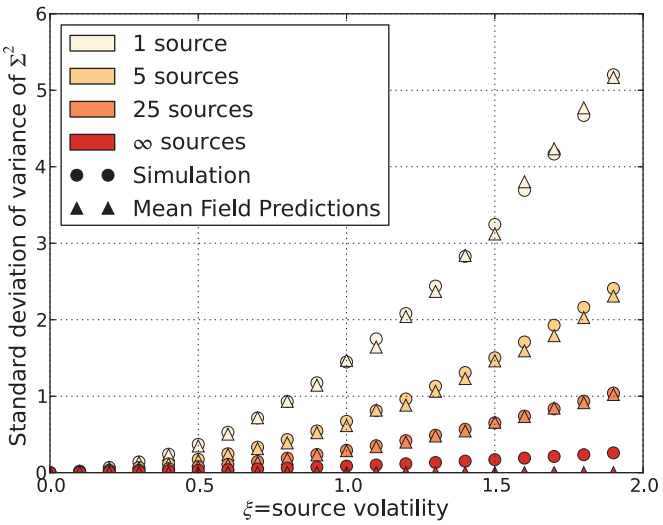


FIG. 4. (Color online) Standard deviation of $\Sigma^2(t)$ as a function of source volatility $\xi$. The normalized gain was chosen to be $g = 0.9$. Reservoirs of size $N = 500$ with $K = 1,5,25,500$ independent and identically distributed Gaussian source with total variance $\xi^2$ were simulated according to Eqs. (1) and (3). The reservoirs were run for 200 time steps to eliminate transitory effects, and then the variance $\Sigma^2(t)$ of the activation potential was recorded for 2000 time steps. The standard deviation (over time) of $\Sigma^2(t)$ was computed and is plotted in the figure using dots. This is compared the predictions of the mean-field theory [Eq. (8)], plotted using triangles. Note that the mean-field predictions go to zero as $K \to \infty$, but we cannot have more than 500 sources for a reservoir of this size.

source terms, then the variance of the time-dependent source term $v_K^2(t)$ in the mean-field equations (8) decreases. In the limit $K \to \infty$, the source term becomes time independent. This is the form of the mean-field equation that obtains in the case of independent inputs, Eq. (4).

We now discuss in a little more detail the later case of independent inputs [Eq. (4)]. This corresponds to a time-independent source term in Eq. (8): $v_K^2(t) = \xi^2$. The recurrence equation (8) then admits a stationary solution. When $\xi^2 > 0$, the stationary solution of Eqs. (8) always differs from zero: $\sigma^2 > 0, \Sigma^2 > 0$. For very small gain $g \to 0$ we have $\Sigma^2 = \xi^2$, $\sigma^2 = F(\xi^2)$. For large gain $g \to \infty$ the stationary solution tends to the solution in the absence of source $\sigma^2 \to 1$, $\Sigma^2 \to g^2$.

In Fig. 4 we compute the standard deviation of $\Sigma^2(t)$ of an echo state network driven by one source, by multiple source, and in the case of independent sources, as a function of the source volatility $\xi^2$. We compare the predictions of the mean-field theory [Eq. (8)] and of the exact equations (1)–(4).

## V. STABILITY

The mean-field theory also allows a derivation of the Lyapunov exponents of the echo state network (see Refs. [3,5,17] for related earlier work). For simplicity we discuss only the case of a single input. Suppose that an echo state network is run until it reaches a typical state. At some time, say, $t = 0$, the solution is slightly perturbed and then allowed to evolve. We therefore have two neighboring solutions $a_i(t)$ and $a_i'(t)$. Denote by $\delta(t) = a_i(t) - a_i'(t)$. The

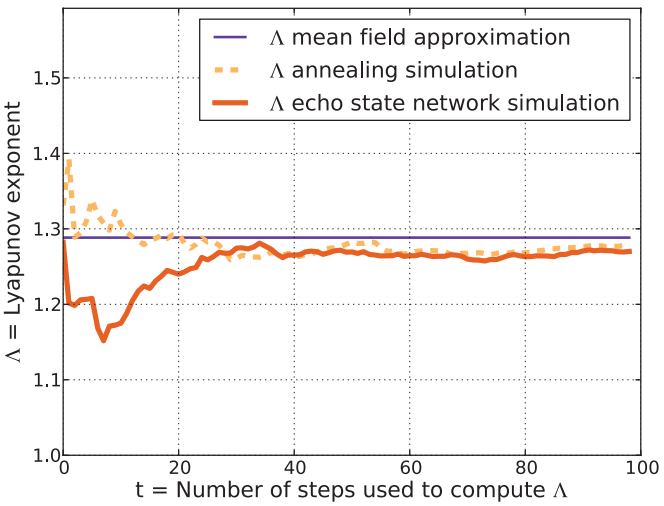


FIG. 5. (Color online) Convergence of Lyapunov exponent estimate. A single reservoir of size $N = 500$, normalized gain $g = 2$, and source variance $\xi^2 = 0.2$ was run for 200 steps. Then the states were perturbed with independent and identically distributed Gaussians with standard deviation $10^{-10}$ and the size of the perturbation was recorded for 100 time steps. The Lyapunov exponent $\Lambda$ was computed for the different lags: $\sqrt[t]{\delta^2(t)/\delta^2(0)}$. The solid dark gray (red) line is the result of a simulation done according to Eqs. (1) and (2), the dotted light gray (orange) line is the result of a simulation done in the annealed approximation, and the straight dark gray (blue) line is the mean-field theory prediction computed from (10).

largest Lyapunov exponent of the system is given by $\Lambda = \lim_{t\to\infty,\delta(0)\to 0} \sqrt[t]{\delta^2(t)/\delta^2(0)}$.

The mean-field theory allows one to evaluate the largest Lyapunov exponent $\Lambda$. We suppose that the two neighboring solutions $a_i(t)$ and $a_i'(t)$ have joint Gaussian distribution:

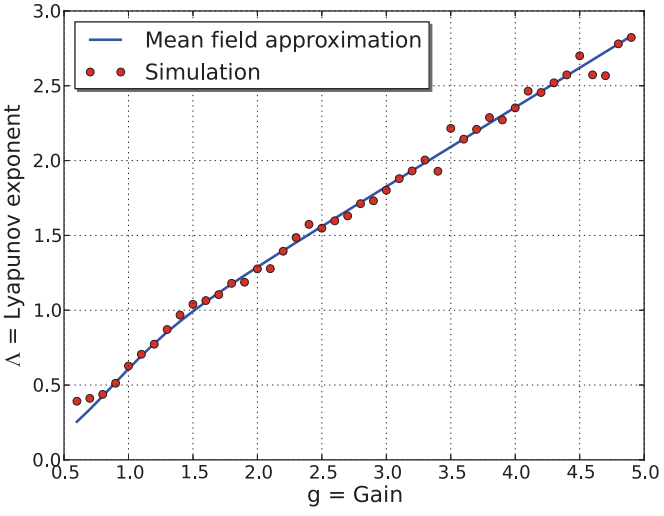


FIG. 6. (Color online) Lyapunov exponent as a function of gain. An $N = 500$ reservoir with source variance $\xi^2 = 0.2$ was run for 200 time steps and then perturbed by independent and identically distributed Gaussians with standard deviation $10^{-12}$ and run for 20 time steps. The Lyapunov exponent was computed based on how much the perturbation changed and is plotted in dark gray (red) dots. The mean-field theory prediction is shown in a solid gray (blue) line.

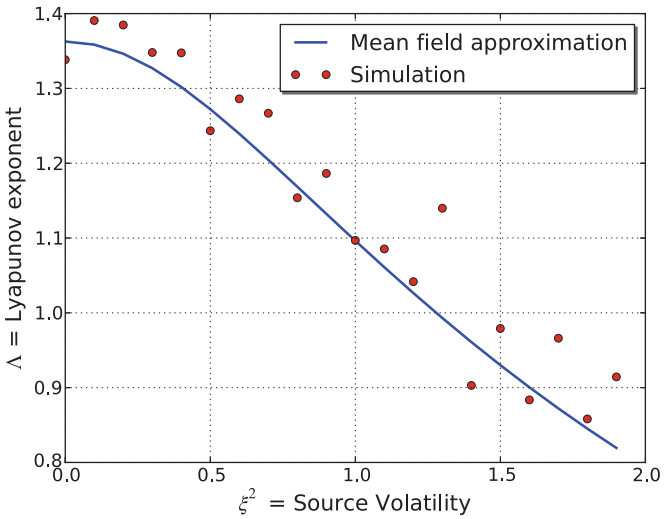


FIG. 7. (Color online) Lyapunov exponent as a function of source volatility. An $N = 500$, $g = 2$ reservoir was run for 200 time steps and then perturbed by independent and identically distributed Gaussians with standard deviation $10^{-12}$ and run for 20 time steps. The Lyapunov exponent was computed based on how much the perturbation changed and is plotted in dark gray (red) dots. The mean-field theory prediction is shown in a solid gray (blue) line.

$\frac{a_i(t)+a_i'(t)}{2} \sim N(0, \Sigma^2(t))$, $a_i(t) - a_i'(t) \sim N(0, \delta^2(t))$. We take $\delta^2(t)$ small and wish to compute how it evolves with time. We have

$$\begin{aligned} a_i(t+1) - a_i'(t+1) &= \sum_j w_{ij} f'\left[\frac{a_i(t)+a_i'(t)}{2}\right][a_i(t) - a_i'(t)] \\ &\quad + O[(a-a')^2], \end{aligned} \tag{9}$$

where $f' = df(a)/da$ is the derivative of $f$ with respect to its argument. From this equation we derive that

$$\begin{aligned} \delta^2(t+1) &= \delta^2(t)\Lambda(\Sigma^2(t)) + O(\delta^3(t)) \\ \Lambda(\Sigma^2) &= g^2 \int da\ f'^2(a) \frac{\exp\left[-\frac{a^2}{2\Sigma^2}\right]}{\sqrt{2\pi\,\Sigma^2}}. \end{aligned} \tag{10}$$

In Fig. 5 we compare the Lyapunov exponents computed from the exact equations of motion and from the mean-field theory.

From expression (10) we deduce two interesting properties. First, in the absence of source, the quiescent stationary solution $\sigma^2(t) = \Sigma^2(t) = 0$ has the largest Lyapunov exponents smaller than 1 for $g < 1$ and the largest Lyapunov exponents larger than 1 for $g > 1$. [This follows from the fact that the integral in Eq. (10) equals 1 in the limit $\Sigma^2 \to 0$, since $f'(0) = 1$.] Thus, in the absence of source, $g = 1$ is the threshold for chaos in the dynamical system.

Second, for sigmoidal functions $f$, we find the property (well known to those who use echo state networks for machine learning tasks; see, e.g., Ref. [16]) that increasing the strength of source term $\xi^2$ stabilizes the system. Indeed, when $\xi^2$ increases, $\Sigma^2$ also increases. For sigmoidal functions $f'(a)$ is a decreasing function of $|a|$, and, hence, the integral in Eq. (10) decreases when $\Sigma^2$ increases. See Figs. 6 and 7 for illustrations of this prediction.

## VI. CONCLUSION

In the present work we have shown that mean-field theory can be applied to large random networks driven by external signals. The agreement, at least in the specific case of echo state networks, with the exact integration of the equations of motion is remarkably good, as illustrated by the figures.

The mean-field theory itself is closely related to the annealed approximation wherein the $w_{ij}(t)$ and the $u_i(t)$ are redrawn independently at random at each time $t$ from the same distribution, i.e., the coupling coefficients become time dependent; see Eq. (5). We expect the mean-field theory to be exact in the large $N$ limit of the annealed approximation.

Compared with the case when there is no external signal, we recover a number of features which are well known empirically to people working with echo state networks but which have not been derived analytically before. In particular, we find that if in the absence of external signal the system has a trivial stable state (corresponding in our analysis to the case $g < 1$), then in the presence of external signal the dynamics becomes nontrivial. We also find that the presence of the external signal tends to stabilize the system (i.e., Lyapunov exponents which decrease when the external signal increases).

We also compare the cases where the dynamical system is driven by independent input signals and by a single or a small number of input signals. We find a qualitative difference, namely, in the first case, the mean-field theory predicts that the collective variables take on stationary values, whereas, in the second case, the mean-field theory predicts their statistical distribution.

The present work should provide the basis for further development of the theory of dynamical systems in the highly important case in practice when they are driven by time-dependent external signals.

## ACKNOWLEDGMENTS

We acknowledge funding from the FRS-FNRS, the IAP under project Photonics@be, and the Action de Recherche Concertée.

[1] D. J. Amit and M. Tsodyks, Network **2**, 259 (1991).
[2] A. Treves, Network **4**, 259 (1993).
[3] B. Cessac, J. Phys. I **5**, 409 (1995).
[4] M. Mattia and P. Del Giudice, Phys. Rev. E **66**, 051917 (2002).
[5] H. Sompolinsky, A. Crisanti, and H. J. Sommers, Phys. Rev. Lett. **61**, 259 (1988).
[6] O. Moynot and M. Samuelides, Probab. Theory Relat. Fields **123**, 41 (2002).
[7] B. Lindner, J. Garcia-Ojalvo, A. Neiman, and L. Schimansky-Geier, Phys. Reports **392**, 321 (2004).
[8] F. Sagues, J. M. Sancho, and J. Garcia-Ojalvo, Rev. Mod. Phys. **79**, 829 (2007).

[9] O. Faugeras, J. Touboul, and B. Cessac, Front. Comput. Neurosci. **3**, 1 (2009).
[10] J. Touboul, G. Hermann, and O. Faugeras, SIAM J. Appl. Dyn. Syst. **11**, 49 (2012).
[11] H. Jaeger, Fraunhofer Institute for Autonomous Intelligent Systems Technical Report, GMD Report 148, 2001.
[12] H. Jaeger and H. Haas, Science **78**, 78 (2004).
[13] W. Maas, T. Natschlager, and H. Markram, Neural Comput. **14**, 2531 (2002).
[14] D. Verstraeten, B. Schrauwen, M. D. Haene, and D. Stroobandt, Neural Networks **20**, 391 (2007).
[15] M. Lukoševičius and H. Jaeger, Comput. Sci. Rev. **3**, 127 (2009).
[16] Mantas Lukoševičius, in *Neural Networks: Tricks of the Trade*, Vol. 2 (Springer, Berlin, 2012), pp. 659–686.
[17] A. S. Pikovsky, Phys. Lett. A **165**, 33 (1992).
[18] E. Ott, C. Grebogi, and J. A. Yorke, Phys. Rev. Lett. **64**, 1196 (1990).
[19] B. Schrauwen, L. Büsing, and R. Legenstein, Adv. Neural Inform. Process. Syst. **21**, 1425 (2009).
[20] M. Hermans and B. Schrauwen, Neural Comput. **24**, 104 (2012).
[21] C. K. A. Williams, Neural Comput. **10**, 1203 (1998).
[22] D. V. Buonomano and W. Maass, Nat. Rev. Neurosci. **10**, 113 (2009).
[23] B. Derrida and Y. Pomeau, Europhys. Lett. **1**, 45 (2007).
[24] N. Bertschinger and T. Natschläger, Neural Comput. **16**, 1413 (2004).
[25] Y. Paquot *et al.*, Sci. Rep. **2**, 287 (2012).
[26] L. Larger *et al.*, Opt. Express **20**, 3241 (2012).